ISSN: 2277-9655
Impact Factor: 5.164
CODEN: IJESS7

IJESRT
INTERNATIONAL JOURNAL OF ENGINEERING SCIENCES & RESEARCH TECHNOLOGY

VISIBLE LIGHT DRIVEN PHOTOCATALYTIC ACTIVITY PERFORMANCE OF FE DOPED CDS NANOPARTICLES BY WET CHEMICAL ROUTE

N. Jeevanantham, M. Elango, O.N. Balasundaram*
[a]Department of Physics, PSG College of Arts and Science, Coimbatore – 641 014, Tamilnadu, India

DOI: 10.5281/zenodo.1184062

ABSTRACT

Nanocrystalline Fe doped CdS nanoparticles were successfully synthesized by wet chemical method. The concentration of Fe is varied from 5 to 15 mol.%. The role of Fe dopant on structural, morphological and optical properties of the ZnO nanoparticles has been analyzed through X-ray diffraction (XRD), transmission electron microscope (TEM), UV-Vis absorption spectra and photoluminescence spectra analysis. Powder XRD results suggest that Fe doped CdS samples showed cubic structure and the results are good in agreement with the standard JCPDS value (card no. 80-0019). Nanocrystalline spherical shaped morphology with average diameter of around 25-15 nm was observed through TEM images. A considerable red shift in the absorption edge and surface related defects were observed by UV and PL analysis. The photocatalytic activities of Fe doped CdS were evaluated by irradiating the solution of methylene blue (MB) and rhodamine B (RHB) under visible light. The results suggest that Fe doped CdS (15 %) showed highest photocatalytic efficiency compared other samples. The improved photocatalytic mechanism by Fe doped was also discussed in detail.

KEYWORDS: Fe doped CdS, semiconductors, transmittance microscope, optical property, visible light, catalyst

I. INTRODUCTION

Environmental harms related with organic pollutants and toxic water pollutants offer the impulsion for sustained essential and applied research in the area of environmental remediation [1]. Recently, semiconductors photocatalysis are being considered for the elimination of organic and inorganic pollutants from aqueous dye solutions [2]. Nowadays, cadmium sulphide (CDS) has paid much attention for the degradation of organic pollutants owing to the excitation of holes and electrons by illumination of visible light [3-7]. CdS is one of the most important semiconductor with direct-band-gap of 2.42 eV [8]; so it has a promising potential application in electroluminescent, photoluminescent and photoconductive devices [9-12]. Moreover, a suitable band gap and high visible absorption property of CdS has been considered as the excellent photocatalyst to degrade the dyes like Rhodamine B (RhB) and Methylene blue (MB) [13-15]. However, decreasing the particle size of a photocatalyst also increases the rate of surface charge recombination. As a result, the activity of particulate photocatalyst does not increase monotonically with decreasing particle size. Generally, doped method is suitable technique to modified the electronic structure and size of the pure CdS nanoparticles. Many metals (Fe, Co, Ni and Zn) have been doped with CdS to enhancing the visible light photocatalytic properties of pure CdS. Recently, Fe doped CdS has been investigated due to their suitable physic-chemical and magnetic properties. CdS with Fe^{2+} in visible light produces electrons and holes; some of the holes are trapped by the Fe^{2+} centers converting them to Fe^{3+} centers. It is well known that iron acts as a killer centre in cadmium sulphide and quenches luminescent properties. Hence, in the present work Fe dopant has been used to enhance the visible light photocatalytic properties of CdS. The role of Fe dopant on structural, optical and photocatalytic properties of CdS has been systematically investigated. The Fe doped CdS showed highest degradation efficiency (91 %) towards MB dye solution. To the bestof the author's knowledge this is the first preliminary report about high performance photocatalytic properties of Fe doped CdS nanoparticles by simple wet chemical method.

ISSN: 2277-9655
Impact Factor: 5.164
CODEN: IJESS7

II. MATERIALS AND METHODS

2.1. Materials

Cadmium acetate dehydrate $Cd(CH_3COO)_2.2H_2O$, sodium sulfide ($Na_2S.2H_2O$), ferrous sulfate ($FeSO_4 \cdot 2H_2O$) for source materials for CdS and Fe respectively. The chemicals were purchased from Merk, India. All the chemicals used were of analytical grade and were used as received without any further purification.

2.2. Preparation of Fe doped CdS

In the typical experimental procedure, 2 gm of Cd and S precursors were dissolved in ethanol in 200 ml beaker separately and were added drop wise under strong magnetic stirring. Ferrous precursor (5 to 15 mol%) was added in to this solutions after the 30 min of vigorous stirring. To this mixture, 20 ml of ethanol was further added and allowed for 6 h stirring. The NH_4OH (as precipitate agent) solution was added drop wise until the pH value reaches to 11. During this process the drop rate must be controlled in order to maintain the chemical homogeneity. The entire solution turned into deep green in color and further allowed to stirrer for 48 h which in optimized aging period of the growth process. The dark green final products were washed thoroughly with the organic solvents (acetone, ethanol) and dried at 160 ^oC in a hot air oven and preserved in moisture free container.

2.3. Characterization techniques

The structure and average grain size of the samples were analyzed by using X-ray patterns of the powders were recorded using a Bruker D8-ADVANCE diffractometer (Cu Kα radiation: λ =1.5418 $^\circ$A). TEM was recorded with JEM2100 model. High resolution electron microscope was recorded with accelerating voltage of 200 kV. The elemental analysis of the samples was analyzed by EDS spectra (JEOL Model JED – 2300). UV-VIS absorption spectra were taken on a Perkin-Elmer Lambda 2 spectro-meter. Photoluminescence spectra of the samples were recorded using PerkinElmer LS 55 spectrometer equipped with a He-Cd laser source, Excitation length used was 325 nm. The functional groups were analyzed by suing Fourier transformed infrared spectra (FT-IR), which is collected using a 5DX FTIR spectrometer.

2.4. Photocatalytic setup

A specially designed photocatalytic reactor system made of double walled reaction chamber of glass tubes was used for photodegradation experiments. A 300W xenon lamp as the light source and the control of the reaction bottle of the plane window 20 cm from the xenon lamp, the reaction using 420 nm high pass filter to remove the ultraviolet light. The photocatalytic degradation reactions of MB and RHB were considered from the model pollutants. The 50 mg of the prepared photocatalyst was mixed with 50 *mL* of aqueous solution containing the appropriate dye (10*mg/L* for MB and RHB). Prior to reactions, the dye solution with catalysts was stirred in the dark for 30 min to attain the adsorption, desorption equilibrium. The concentration of the aqueous suspensions (MB and RHB) in each sample was analyzed using UV–Vis spectrophotometer at a wavelength of 664 nm. The photocatalytic efficiency was calculated from the expression $\eta = (1-C/C_0)$, where C_0 is the concentration of dyes (MB and RHB) before illumination and C is the concentration of dyes after a certain irradiation time. The time interval of irradiation time was 20 min.

III. RESULTS AND DISCUSSION

3.1 XRD analysis

The structure and average grain size of the as synthesized samples were analyzed through XRD. Fig.1 shows the powder XRD pattern of Fe doped CdS powders with different Fe contents. The reflection peaks of as synthesized powders can be indexed to be cubic phase, has three main peaks at 30.62°, 51.32° and 62.09°, which is corresponding reflections of (111), (220) and (311) planes. The results are good in agreement with the standard JCPDS value (card no. 80-0019). No other impurity peaks were detected in the spectra, this result suggests that Fe dopant is distributed homogenously without clustering or segregation [16]. Moreover, the

ISSN: 2277-9655
Impact Factor: 5.164
CODEN: IJESS7

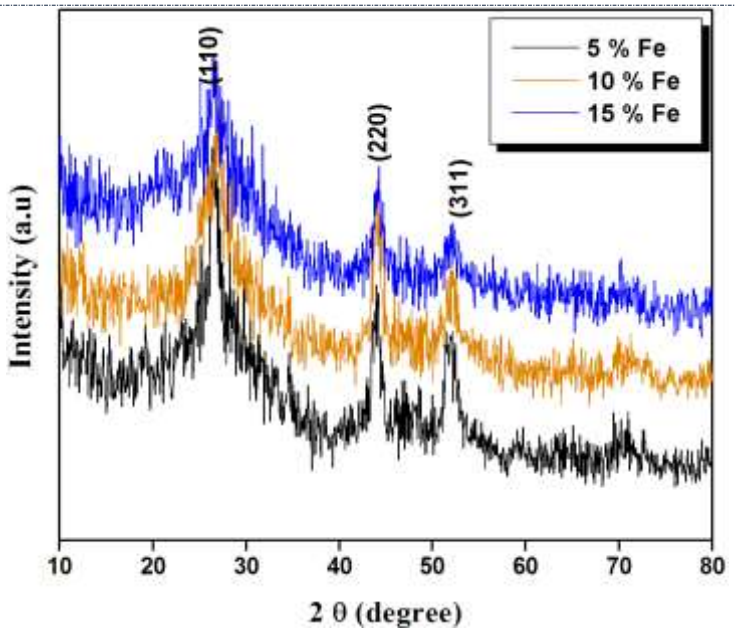

Fig.1. Powder XRD pattern of Fe doped CdS nanoparticles

Diffraction peak intensity was increased and shifted towards the higher angle side with the increase of Fe content. In addition, the average grain size and lattice parameters values were decreases with the increase of Fe concentrations (Table. 1). This may be due to the smaller ionic radius of Fe^{3+} (0.064 nm) compared to Cd^{2+} (0.096 nm).

The average crystalline sizes of the Fe doped CdS nanoparticles were calculated by using Scherrer's equation [17].

$$d = \frac{K\lambda}{\beta \cos\theta}$$

Where d is the mean crystallite size, K is the shape factor taken as 0.89, λ is the wavelength of the incident beam, β is the full width at half maximum and θ is the Bragg angle. The average crystalline size was calculated as 24 nm, 20 nm and 17 nm for Fe doped CdS nanoparticles were respectively. This result suggests that the grain growth is reduced due to doping of Fe into Cd-site.

3.2. Transmission electron microscope analysis

TEM is a useful technique to determine the surface morphology and average particle size of the samples. Fig.2 (a-c) shows the TEM images of Fe doped CdS nanoparticles. Fe-doped CdS nanoparticles reveal a spherical morphology having uniform particle size. Fe doping decreases the average size of CdS nanoparticles with increase of Fe content. The average particle sizes were around 25 to 15 nm, which is in good agreement with the grain size calculated from XRD results. HRTEM images of 15% Fe doped CdS nanoparticles reveals that the nanocrystals are cubic with a d-spacing value of 0.33 nm, corresponding to the (111) plane (fig 2 d). The corresponding SAED patterns show sharp and circular rings indicating that the nanoparticles are of polycrystalline nature (inset fig 2 d). In order to verify the compositional elements present in the samples, EDS analysis was carried out for 15% Fe doped CdS nanoparticles and the spectra was presented as shown in Fig. 2e. The samples mainly composed of Cd, Fe and S and did not show any traces of other elements. The calculated compositional ratio of Cd/Fe in the nanocrystals is approximately same as that of the reactants ratio over a large composition range. The Cu element was found in the composition, due to the grid used for EDS measurements.

ISSN: 2277-9655
Impact Factor: 5.164
CODEN: IJESS7

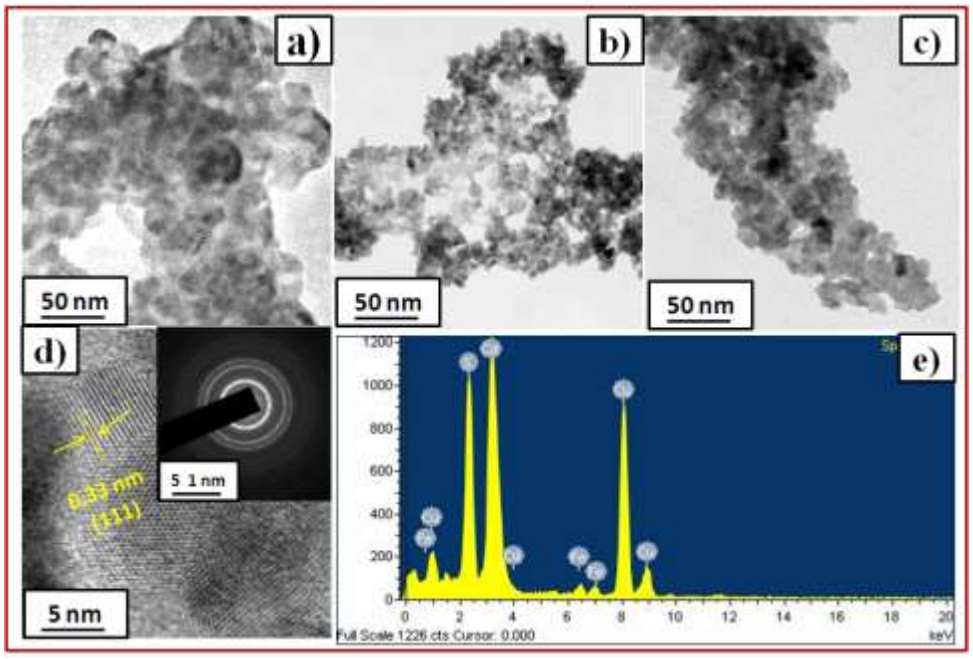

Fig.2. TEM images of a) 5 % Fe b) 10 % Fe c) 15 % Fe d) high resolution TEM images of 15 % Fe and SAED pattern (insert) e) EDS spectra of 15 % Fe doped CdS nanoparticles

3.3. UV-Vis absorption spectra analysis

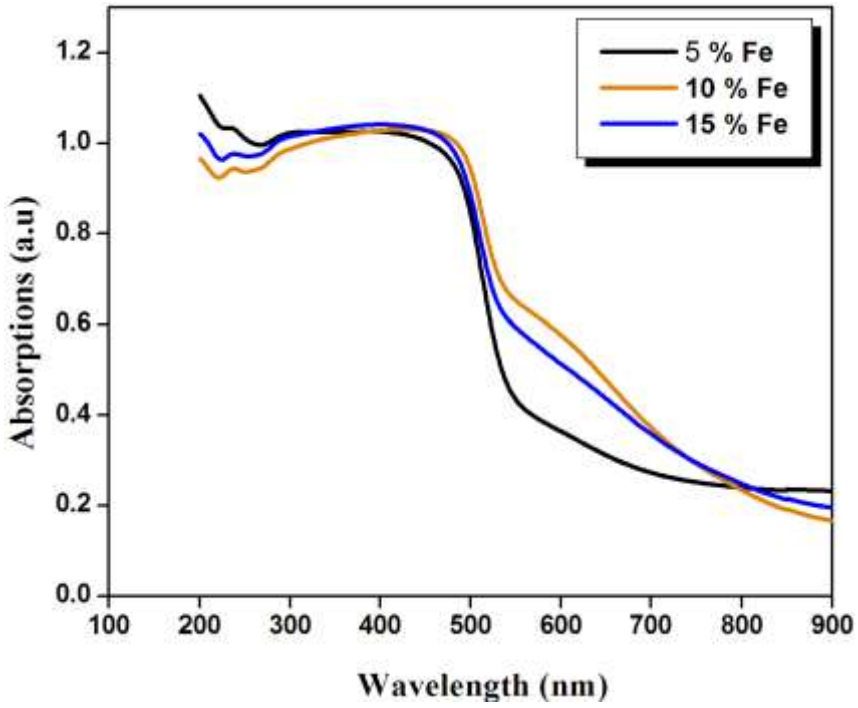

Fig.3. UV-Vis absorptions spectra of Fe doped CdS nanoparticles

ISSN: 2277-9655
Impact Factor: 5.164
CODEN: IJESS7

The optical property and band gap energy of the samples were analyzed by UV-Vis absorption spectra. Fig.3 shows the UV-Vis absorption spectra analysis of Fe doped CdS nanoparticles with different Fe content. It can be seen that the intensive absorptions are present in ultraviolet–visible range of about 250–510 nm. It was clear evident that the absorption edge was shifted towards the higher wavelength with the increase of Fe content. A considerable red shift in absorption edge was indicates that decreasing the bang gap energy. The absorption coefficient (α) was calculated from the transmission spectra using equation [18],

$$\alpha = 1/t \ln(1/T)$$

Where T is the optical transmission and t is the thickness of the samples. The direct band gap of the Fe doped CdS nanoparticles was analyzed by using the relation [19].

$$\alpha h\nu = A(h\nu - E_g)^m$$

Where α is the absorption coefficient, h is the Planck's constant, ν is the frequency of incident light, E_g is the energy band gap of material and m is the factor governing the direct, etc. The band gap energy was calculated as 2.51 eV, 2.45 eV and 2.36 eV for Fe (5, 10 & 15%) doped CdS samples respectively. The decreasing in the band gap values of some samples such as CdS doped Fe was due to the new energy levels introduced in the host lattice upon doping [20,21]. Where the introduced of Fe^{3+} in CdS lattice decreased crystallite sizes while the band gap also decreased.

3.4. Photoluminescence spectra analysis

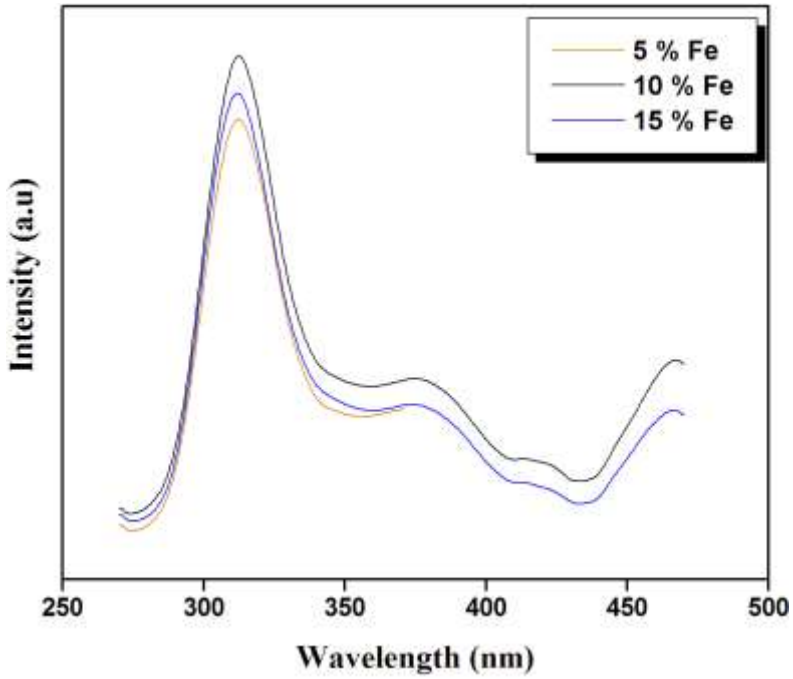

Fig.4. Photoluminescence spectra of Fe doped CdS nanoparticles

Photoluminescence is a commonly used tool for probing electron-hole surface processes of semiconductor materials, the determination of band-gap energy and surface defect in the samples [22]. Fig. 4 shows the PL emission spectra of Fe doped CdS nanoparticles with different Fe content measured from 300 to 600 nm using a 325 nm He–Cd laser. A strong UV emission peak was observed for all the cases. This may be due to the surface defect, band gap decreasing and vacancy (Vs) of the samples during the synthesis process. When the Fe content increases, the peak intensity was decreased with shifted towards the longer wavelength. This result suggests that decreasing band gap and improves the optical property of CdS by Fe doping.

ISSN: 2277-9655
Impact Factor: 5.164
CODEN: IJESS7

3.5. FTIR spectra analysis

Fourier Transform Infrared (FTIR) Spectroscopy is a technique that provides information about the chemical bonding or molecular structure of materials. Fig. 5 shows FTIR spectra of Fe doped CdS nanoparticles with different Fe content in room temperature. It can be seen that in the higher energy region the peak around at 3423 cm^{-1} is attributed to O-H stretching and the peak appeared at 1614 cm^{-1} is assigned to bending (H-O-H) vibration of the water absorbed on the surface of CdS [23]. The sharp peak around at 1422 cm^{-1} is assigned to bending vibration of ethanol used in the process. The C-O stretching vibration of absorbed methanol gives peak at 1098 cm^{-1}. The absorption band at 663 cm^{-1} has been assigned to CdS stretching [24]. There is no vibration for Fe related to peaks, this results again supported that Fe has successfully doped with CdS nanoparticles.

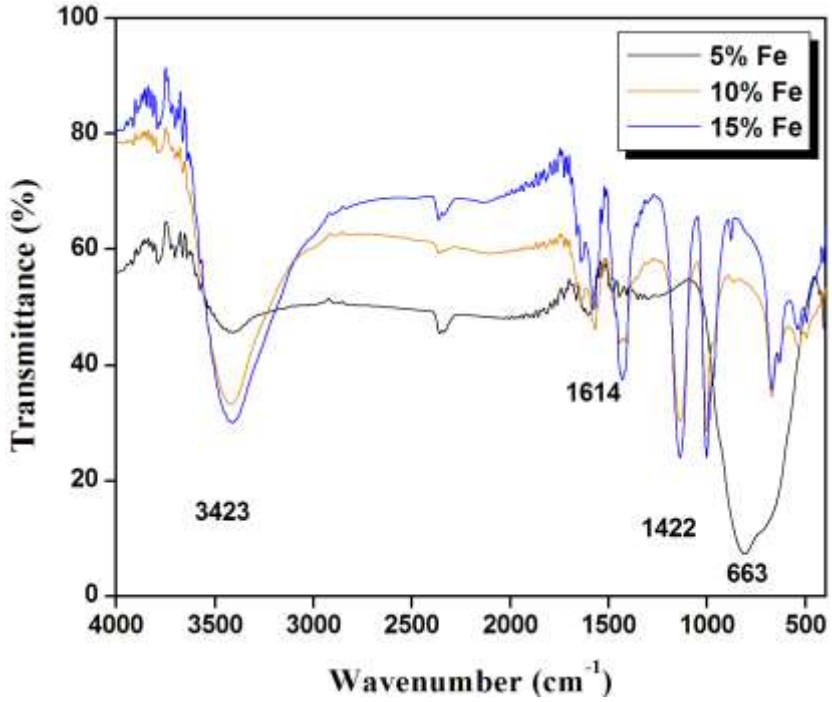

Fig.5. FTIR spectra of Fe doped CdS nanoparticles

3.6. Photocatalytic studies

3.6.1. Absorbance and visible light driven photocatalytic test

The catalytic effect of the material was examined by monitoring the intensity of absorption and emission peaks with irradiation time. The absorption spectra of the aqueous solution of MB and RhB dyes were irradiated under visible light are recorded at the time interval of 20 min and shown in Fig. 6 a)-d). It was clear evident that the intensity of absorbance was drastically decreases with the increase of irradiation time. The intensity of all the samples was completely disappearing in 120 min irradiation of visible light. Hence, we concluded that these samples are more photo active material under visible light conditions. The samples were further tested for photocatlytic efficiency for the degradation of MB and RhB dye solutions under visible light irradiation. Figs.7 & 8 show the temporal degradation profile for Fe doped CdS catalyst powders with MB dye solution under visible light irradiation. It was seen that the degradation rate changed evidently with time increasing when Fe-CdS used as catalyst, and the degradation rate reached the highest at the 100 min. And we can see from Figs. 7 & 8. The degradation efficiency of the MB dye was found to be 67 %, 78% and 89 % for Fe (5, 10 & 15%) doped CdS nanoparticles respectively. similarly, the degradation efficiency of the RhB dye was found to be 71 %, 86 % and 94 % for Fe (5, 10 & 15%) doped CdS nanoparticles respectively. The improved efficiency is attributed to Fe^{3+} dopant can serve as charge traps retarding electron-hole combination rate and thereafter enhancing the interfacial charge transfer for MB & RhB degradation within a suitable molar ratio of Fe^{3+}/Cd^{2+}.

ISSN: 2277-9655
Impact Factor: 5.164
CODEN: IJESS7

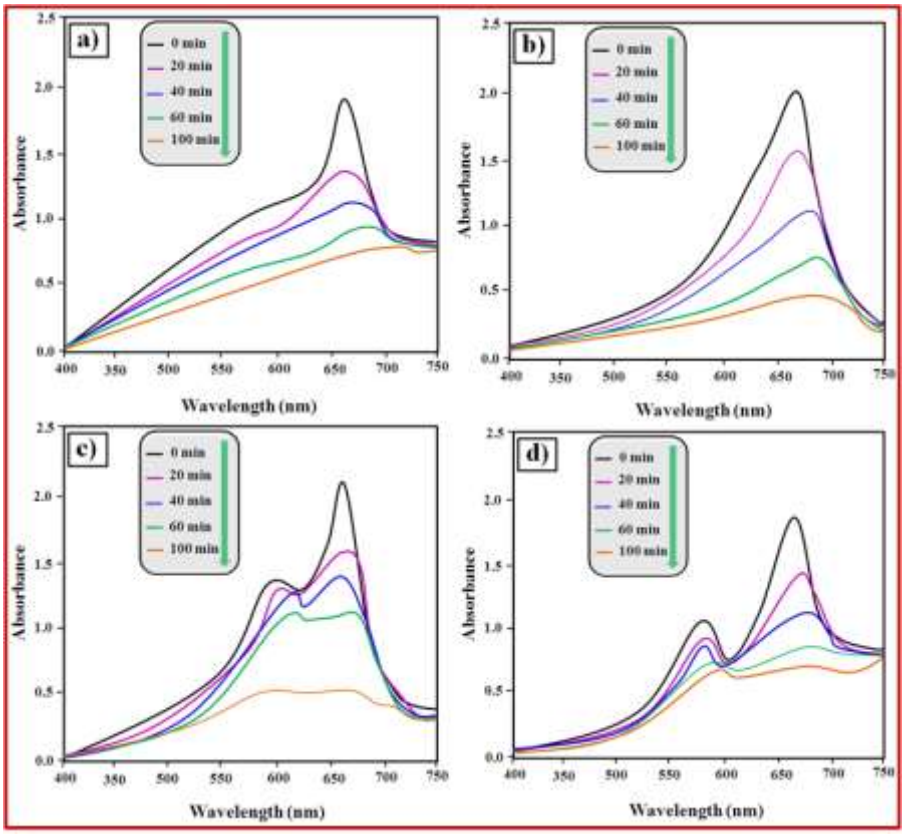

Fig.6. UV absorption spectra of MB dye solution by using a) 5 % Fe and b) 15 % Fe doped CdS nanoparticles; UV absorption spectra of RhB dye solution by using c) 5 % Fe and d) 15 % Fe doped CdS nanoparticles under visible light irradiation

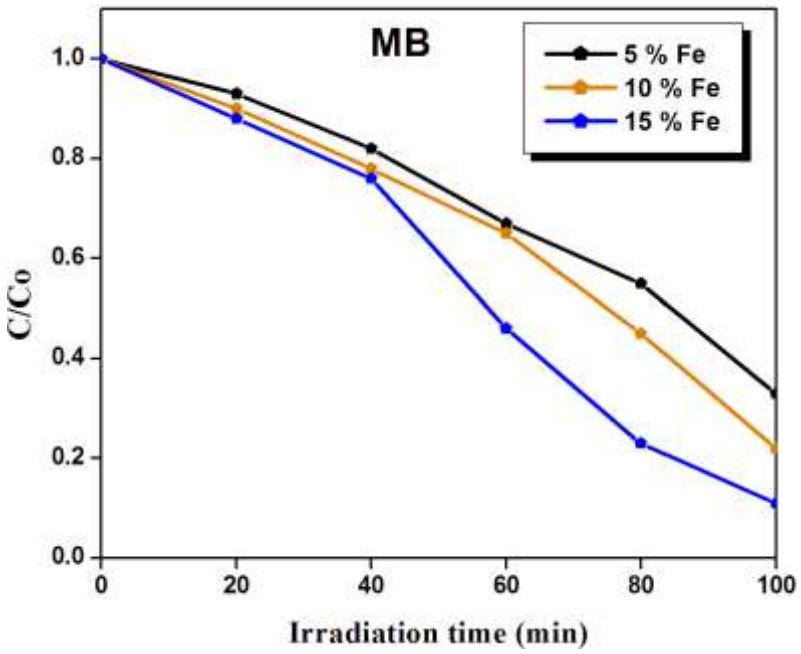

Fig.7. Photocatalytic degradation of MB using Fe doped CdS catalyst under visible light irradiation.

ISSN: 2277-9655
Impact Factor: 5.164
CODEN: IJESS7

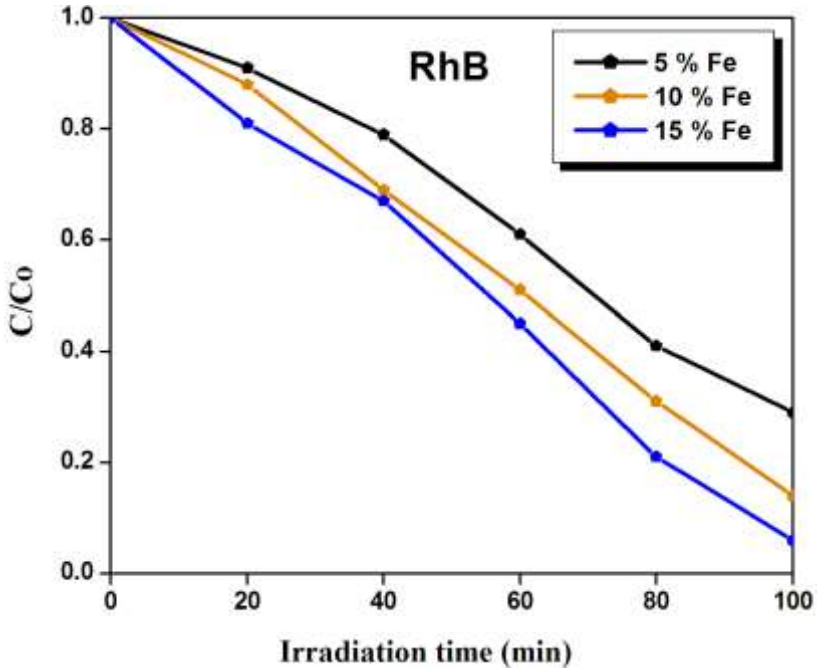

Fig.8. Photocatalytic degradation of RhB using Fe doped CdS catalyst under visible light irradiation.

3.6.2. Recycle test

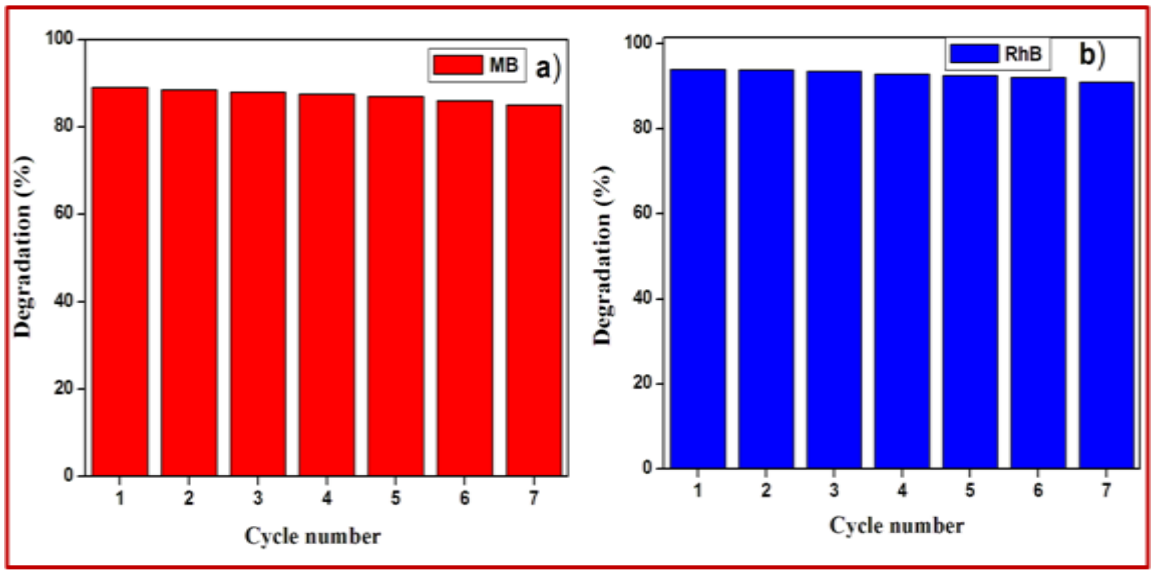

Fig.9. Recycling cycles of test of a) MB and b) RhB using Fe doped CdS catalyst under visible light irradiation.

In practical applications stability and recyclability is most important concern in the photocatalytic test. The samples were further analyzed by recycling test. The reusability of Fe doped CdS catalyst powders was tested by recycling the catalyst under the same condition, and the results are plotted in Figure 9 a) & b). The results show there is a ~4% decrease (89 to 85%) in degradation efficiency for MB, similarly RhB was ~3% decrease (94 to 91%) after seventh cycles. After 7 runs of photodegradation of MB and RhB the photocatalytic activity of the Fe-CdS catalyst shows a small deterioration due to incomplete recollection and loss during the washing

ISSN: 2277-9655
Impact Factor: 5.164
CODEN: IJESS7

process. Therefore, the Fe-CdS catalyst can be preferable for high performance photocatalst and waste water treatment.

3.6.3. Photocatalytic mechanism

The schematic representation of Fe doped CdS under visible light is shown in Fig.10. The improved photocatalytic mechanism of Fe doped CdS is due to Fe^{3+} in CdS can introduce doping energy level on the top of valence band. With the increase of doping concentration, the band gap of Fe-doped CdS becomes narrower, which is beneficial for the generation of more electrons and holes under visible light irradiation. The widening of valence band will suppress the recombination of photogenerated electronsand holes, facilitating the prolongation of photogenerated carrier life-span. Therefore, much more photogenerated carriers can transfer to the surface than pure CdS and then oxidative radicals (h^+, $^*O_2^-$, $^*OH$) are produced in large quantities. The electron transfers to the adsorbed MB molecule on the particle surface. The excited electron from the photocatalyst conduction band enters in to the molecular structure of MB and complete decomposition of MB. Hole at the valence band generates hydroxyl radical via reaction with water, might be used for the oxidation of other organic compounds. This clearly demonstrates that the Fe doped CdS can be as potential photocatalyst for the water and environmental detoxification from organic pollutants which can operate at visible light

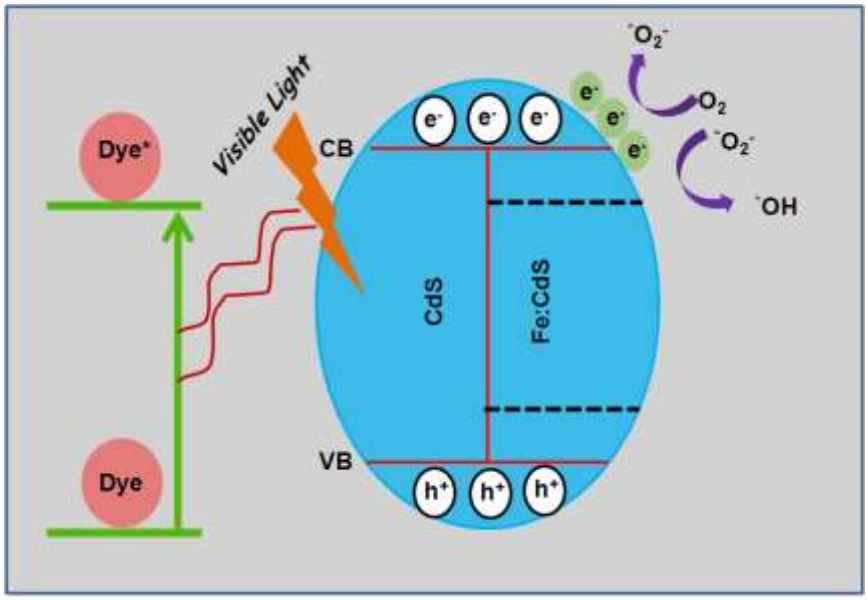

Fig.10. Schematic representation for photocatalytic mechanism of Fe doped CdS catalyst under visible light irradiation.

IV. CONCLUSION

In summary, Fe doped CdS nanoparticles with crystallite size of 24-17 nm have been obtained using the chemical co-precipitation method with NH_4OH as stabilizing agent. The shapes of CdS nanostructures were greatly affected by Fe doping. The incorporation Fe into CdS lattice is confirmed by shifting in the position of XRD and FTIR spectra with increase of Fe content. The EDS spectra further supported that the presence of Fe in the CdS nanocrystal system. The optical measurement yields energy band gaps and reveals that the absorption edge shifted towards the longer wavelength side in Fe doped CdS nanoparticles. The improved photocatalytic activity of Ni doped samples may be due to the presence of doping induced impurity levels within the band gap which may help in prolonging the recombination time of electrons and holes, resulting enhanced photocatalytic degradation of MB and RhB dyes under visible light irradiation.

V. REFERENCES

[1] M.R. Hoffmann, S.T. Martin, W. Choi, D.W. Bahnemann, "Environmental applications of semiconductor photocatalysis", Chemical Reviews, vol. 95, pp. 69–96, 1995.
[2] G. Sachin Ghugala, Suresh S. Umarea, Rajamma Sasikala, "A stable, efficient and reusable CdS–SnO_2 heterostructured photocatalyst for the mineralization of Acid Violet 7 dye", Applied Catalysis A General, vol. 496, pp.25-31, 2015.
[3] D.S. Kim, Y.J. Cho, J. Park, J. Yoon, Y. Jo, M. Jung, "(Mn , Zn) Co-Doped CdS Nanowires, Journal

ISSN: 2277-9655
Impact Factor: 5.164
CODEN: IJESS7

of Physical Chemistry C", vol. 111, pp. 10861–10868, 2007.
[4] M. Zhang, M. Wille, R. Rder, S. Heedt, L. Huang, Z. Zhu, S. Geburt, D. Grtzmacher, T. Schpers, C. Ronning, J.G. Lu, "Amphoteric nature of Sn in CdS nanowires", Nano Letter. vol.14, pp. 518–523, 2014.
[5] L. Li, Z. Lou, G. Shen, "Hierarchical CdS nanowires based rigid and flexible photodetectors with ultrahigh sensitivity", ACS Applied Material Interfaces", vol. 7, pp. 23507–23514, 2015.
[6] D.S. Bhatkhande, V.G. Pangarkar, A.A.C.M. Beenackers, "Photocatalytic degradation for environmental applications - A review", Journal of Chemical Technololy and Biotechnololgy", vol. 77, pp.102–116, 2002.
[7] A. Hernandez-Gordillo, A.G. Romero, F. Tzompantzi, R. Gmez, "New nanostructured CdS fibers for the photocatalytic reduction of 4-nitrophenol", Powder Technology, vol. 250, pp. 97-102, 2013.
[8] M. Ueta, H.B. Kanzaki, K. Kobayashi, Y. Toyozawa, E. Hanamura, "Excitonic Processes in Solids, in: Springer Series in Solid State Sciences, vol. 60, Springer, Berlin, 1986.
[9] A. H. Mueller, M. A. Petruska, M. Achermann, D. Werder, E. Akhadov, D. Koleske, M. Hoffbauer, V. I. Klimov, "Multicolor Light-Emitting Diodes Based on Semiconductor Nanocrystals Encapsulated in GaN Charge Injection Layers", Nano Letters, vol. 5, pp. 1039-1044, 2005.
[10] Z.K. Heiba, M.B. Mohamed, N.G. Imam, "Fine-tune optical absorption and light emitting behavior of the CdS/PVA hybridized film nanocomposite", Journal of Molecular Structure, vol. 1136, pp. 321-329 2017.
[11] N.G. Imam, M.B. Mohamed, "Environmentally friendly $Zn_{0.75}Cd_{0.25}S$/PVA heterosystem nanocomposite: UV-stimulated emission and absorption spectra", Journal of Molecular Structure. Vol. 1105, pp. 80-86, 2016.
[12] Z.K. Heiba, M.B. Mohamed, N.G. Imam, "Hybrid luminescent CdS@ ZnS nanocomposites", Ceramic International, vol. 41, pp. 12930-12938, 2015.
[13] B. Kaur, K. Singh, A.K. Malik, "Precursor dependent morphological and photo-catalytic behaviour of CdS nanostructures", Dyes and Pigments, vol. 137, pp. 352–359, 2017.
[14] X. Yang, Z. Wang, X. Lv, Y. Wang, H. Jia, "Enhanced photocatalytic activity of Zn-doped dendritic-like CdS structures synthesized by hydrothermal synthesis", Journal of Photochemistry and Photobiology A Chemistry, vol. 329, pp. 175-181, 2016.
[15] S. Sankar, S.K. Sharma, N. An, H. Lee, D.Y. Kim, Y.B. Im, Y.D. Cho, R.S. Ganesh, S. Ponnusamy, P. Raji, L.P. Purohit, "Photocatalytic properties of Mn-doped NiO spherical nanoparticles synthesized from sol-gel method", Optik, vol. 127, pp. 10727-10734, 2016.
[16] K. Nomura, C.A. Barrero, J. Sakuma, M. Takeda, "Room-temperature ferromagnetism of sol-gel-synthesized $Sn_{1-x}{}^{57}Fe_xO_{2-\delta}$ powders", Physical Review B, vol. 75, pp. 184411, 2007.
[17] M. Parthibavarman, K. Vallalperuman, S. Sathishkumar, M. Durairaj, K. Thavamani, "A novel microwave synthesis of nanocrystalline SnO_2 and its structural optical and dielectric properties", Journal of Materials Science: Materials in Electronics. vol. 25, pp. 730-735, 2014.
[18] S.S. Roy, J. Podder Gilberto, "Synthesis and optical characterization of pure and Cu doped SnO_2 thin film deposited by spray pyrolysis", Journal of Optoelectronics and Advanced Materials, vol. 12, pp. 1479, 2010.
[19] D. Madhan, M. Parthibavarman, P. Rajkumar, M. Sangeetha, "Influence of Zn doping on structural, optical and photocatalytic activity of WO_3 nanoparticles by a novel microwave irradiation technique", Journal of Materials Science: Materials in Electronics, vol. 26, pp. 6823-6830, 2015.
[20] Z.K. Heiba, M.B. Mohamed, A.M. Wahba, N.G. Imam, "Structural, Optical, and Electronic Characterization of Fe-Doped Alumina Nanoparticles", Journal of Electronic Materials, vol. 47, pp. 711–720, 2018.
[21] N.G. Imam, M.B. Mohamed, "Optical properties of diluted magnetic semiconductor Cu: ZnS quantum dots, Superlattices and Microstructure", vol. 73, pp. 203-213, 2014.
[22] K. Anandan, V. Rajendran, "Intense photoluminescence emission behavior of pure and doped SnO_2 nanoparticles synthesized via solvothermal technique", Journal of Physical Sciences, vol. 19, pp. 129, 2014.
[23] J. Liu, C. Zhao, Z. Li, J. Chen, H. Zhou, S. Gu, Y. Zeng, Y. Li, Y. Huang, "Low-temperature solid-state synthesis and optical properties of CdS–ZnS and ZnS–CdS alloy nanoparticles", Journal of Alloys and Compounds, vol. 509, pp. 9428- 9433, 2011.
[24] H. Sekhar, D. Narayana Rao, "Spectroscopic studies on Fe3+ doped CdS nanopowders prepared by

ISSN: 2277-9655
Impact Factor: 5.164
CODEN: IJESS7

simple coprecipitation method", Journal of Alloys and Compounds, vol. 517, pp. 103– 110, 2012.

CITE AN ARTICLE

N. Jeevanantham, Elango, M., & Balasundaram, O. N. (n.d.). VISIBLE LIGHT DRIVEN PHOTOCATALYTIC ACTIVITY PERFORMANCE OF FE DOPED CDS NANOPARTICLES BY WET CHEMICAL ROUTE . *INTERNATIONAL JOURNAL OF ENGINEERING SCIENCES & RESEARCH TECHNOLOGY*, *7*(2), 702-712.